

Synthesis and Characterization of Semiconductor Nanomaterials and Micromaterials via Gamma-irradiation Route

Yong Hu,^{1,2} and Jia-Fu Chen^{1,3}

Received March 7, 2007; accepted April 16, 2007; published online May 19, 2007

In this review, we reported our recent studies on controlled growth of sulfide and oxide semiconductor nano- and micro-structures via gamma-irradiation route. NiS and PbS uniform hollow microspheres (~500 nm) have been successfully synthesized by γ -irradiating PMMA-CS₂-ethanol aqueous solution that contains Ni²⁺ or Pb²⁺ at room temperature, respectively. Large-scale single-crystalline ZnO hexangular prisms were successfully prepared through a simple γ -irradiation approach at room temperature and under ambient pressure. CdSe hollow structures and hollow nanospheres (40~50 nm), compass-shaped (80 nm in middle width and 200 nm in length) Mn₃O₄ (hausmannite) and monodisperse ZnS nanoballs etc. had been successfully synthesized through γ -irradiation route with different surfactant-assisted systems at room temperature. Those successful synthesis approaches in large scale and under mild conditions could be of interest for both applications and fundamental studies.

KEY WORDS: Semiconductor; nanomaterials; shape-controlled; gamma-irradiation.

INTRODUCTION

Recent advances in the fabrication of semiconductor nano-structures (such as molecular beam epitaxy and metal organic vapor-phase epitaxy) make it possible to construct semiconductor nano-scale objects with a wide range of

¹Hefei National Laboratory for Physical Sciences at Microscale, University of Science and Technology of China, Hefei, Anhui, 230026, P. R. China.

²Department of Chemistry, University of Science and Technology of China, Hefei, Anhui, 230026, P. R. China.

³To whom correspondence should be addressed. E-mail: jfchen@ustc.edu.cn

geometries. Semiconducting materials that are processed into freestanding elements such as wires, ribbons, platelets, rods, crystallites, and other shapes gain interesting new properties compared to their bulk counterparts.

For example, they can be dispersed in solution and transferred to virtually any substrate, including low-cost plastics and even paper, both of which are intrinsically incompatible with procedures used to make conventional bulk wafers of most inorganic semiconductors [1–3]. Also, the properties of these elements can depend strongly on their geometry; this attribute offers new application possibilities [4–15]. Many classes of devices can be built with wires, ribbons, or other structures that have aspect ratios large enough to enable easy electrical connection [16]. Up to now, many methods have been proposed to synthesize semiconductor nanomaterials, such as chemical vapor deposition, templates, hydrothermal, wet-chemistry, laser ablation, self-assembled process, etc [17–21].

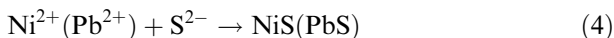
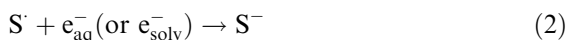
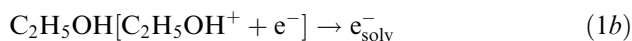
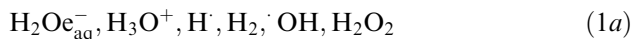
In the last few years, γ -irradiation approach is one of the new and effective methods for synthesis of nanomaterials. This method had been extensively used in the preparation of nanocrystalline metal, alloy, metal oxide, composites, metal sulfide and inorganic/polymer nanocomposites [22–26]. Compared with other methods of preparation of nanomaterials, the γ -ray radiation method can be carried out under ambient pressure at room temperature if wanted. When under irradiation, with isopropanol or 2-methyl-2-propanol as hydroxyl radical(OH) scavenger, the aqueous/ethanol system maintains a reducing atmosphere which reduces high valent metal ion to low valency, thus metal or oxide powders with very small dimensions are obtained. Moreover, when the solution contains the source of sulfur or selenium, it would give out S^{2-} or Se^{2-} under γ -irradiation, then would precipitate with metal cations, so dispersed colloidal sulfide or selenide particles can be prepared by this method. In this review, we try to report our recent studies on controlled growth of sulfide and oxide semiconductor nanostructures via gamma-irradiation approach, such as NiS and PbS uniform hollow microspheres, single-crystalline ZnO hexangular prism, CdSe hollow structures and hollow nanospheres, monodisperse and uniform single-crystal compass-shaped Mn_3O_4 (hausmannite), monodisperse binary ZnS nanospheres, etc [27–32]. They were all successfully synthesized via γ -irradiation route at room temperature.

NiS AND PbS HOLLOW MICROSPHERES

Traditionally, hollow spheres are fabricated by coating the template with a thin shell of the desired materials and subsequently removed template. The difficulties of this method often arise from the control over

the fabrication process, as well as homogeneity and thickness of the coating [33–36].

In order to get highly-dispersed NiS (PbS) hollow spheres, experiments in our method are involving two distinct steps. Firstly, the ethanol aqueous solution containing 40% methyl methacrylate (MMA) monomer was irradiated in the field of γ -ray source at room temperature to obtain transparent polymethyl methacrylate (PMMA) gel. Secondly, PMMA gel was divided into $0.5 \times 1.0 \text{ cm}^2$ /or smaller thin pieces, and then put them into the ethanol solution containing $\text{NiSO}_4 \cdot 6\text{H}_2\text{O}$ [$\text{Pb}(\text{CH}_3\text{COO})_2 \cdot 3\text{H}_2\text{O}$] and CS_2 . While reaching the swelling equilibrium, the solution was also irradiated in the field of ^{60}Co γ -ray source with definite dosage. When the reactions fully finished, it could be got the submicrometer NiS (PbS) spheres. The possible formation mechanism could be explained as follows [37]:



Here, the symbol (\cdot) stands for irradiation; e_{aq}^- and e_{solv}^- represent hydrated electron and solvated electron, respectively.

PMMA has a characteristic behavior, which could be easily degraded by γ -irradiation. While exposure to high-energy radiation, it has been shown degradation in the average molecular weight, with corresponding changes in viscosity and mechanical properties [38, 39]. The key to the successful synthesis of hollow spheres in this experiment is in controlling the radiation-induced degradation of PMMA to MMA monomers, which are insoluble in water and can exist as oil droplets in solution. CS_2 is also insoluble in water and easily adheres to the surface of the MMA oil droplets. As it's designed, these oil droplets (sphere shape) are the reaction centers. Equations 2–4 have taken place on the oil-water (O/W) interface and leading to mineralization around the MMA oil droplets, forming NiS (PbS) sphere with cores of unreacted MMA. Following these, the samples are heated 3 h at 125 °C, the unreacted MMA cores are vaporized, and then leave the NiS shells as

hollow spheres. Our consideration for not directly selecting emulsion or micro-emulsion system is that, if MMA directly being as the oil droplet (oil phase), while gamma ray irradiating, MMA easily polymerized and formed PMMA. This radical chain reaction continued a period, and could not quickly stop. At the same time, S^{2-} formed, in this case, it's impossible for MMA monomer being as the reacting center, but PMMA instead of. Then, a composite sphere with PMMA core might be got.

The surface morphology can be further illustrated by the field emission scanning electron microscope (FESEM, JEOL JSM-6700F SEM, all other FESEM photographs in this article were taken in the same equipment if not especially pointed out) images (Fig. 1). The FE-SEM photographs reveal that the samples consist of uniform monodisperse spheres with 500 nm in diameter. The corresponding transmission electron microscopy (TEM, Hitachi Model H-800, all other TEM photographs in this article were taken in the same setup if not especially explained) image is shown in Fig. 2. This result also confirms that the samples consist of uniform hollow spheres with 500 nm in diameter. The strong contrast between the dark edge and pale center is the evidence for its hollow nature of the spheres [40].

SINGLE-CRYSTALLINE ZnO HEXANGULAR PRISM

Zinc oxide (ZnO) is a unique material that exhibits semiconducting, piezoelectric, and pyroelectric multiple properties because of its wide direct band gap (3.37 eV) and a relatively large excitation binding energy (60 meV). [41–43]. Here, we report a novel approach to prepare monodisperse and uniform large-scale single-crystal ZnO hexangular prism through one-step γ -irradiation route at room temperature and under ambient pressure.

In a typical procedure, analytically pure 0.72 g $ZnSO_4 \cdot 7H_2O$ was dissolved into 50 mL distilled water, 10 mL of 5 M NaOH, 0.8 g Cetyltrimethylammonium Bromide (CTAB) and isopropyl alcohol (15 mL) were added in succession, and then the mixed solution was intensively stirred for 0.5 h at room temperature. Finally, the mixed transparent solution was placed in the field of a 2.22×10^{15} Bq ^{60}Co γ -ray source with the absorption dose of 100 kGy at the dose rate of 50 Gy/min. After irradiation, the white precipitates were collected, washed with ethanol and distilled water several times, then dried in the oven at 60 °C.

FESEM image in Fig. 3a shows that the product is completely composed of hexangular prism with a rim of 230 ± 10 nm and length up to 8.5 μm . The areas of rectangle (Fig. 3a) are shown enlarged in Fig. 3b and 3c. From these, we can further clearly see that the samples are

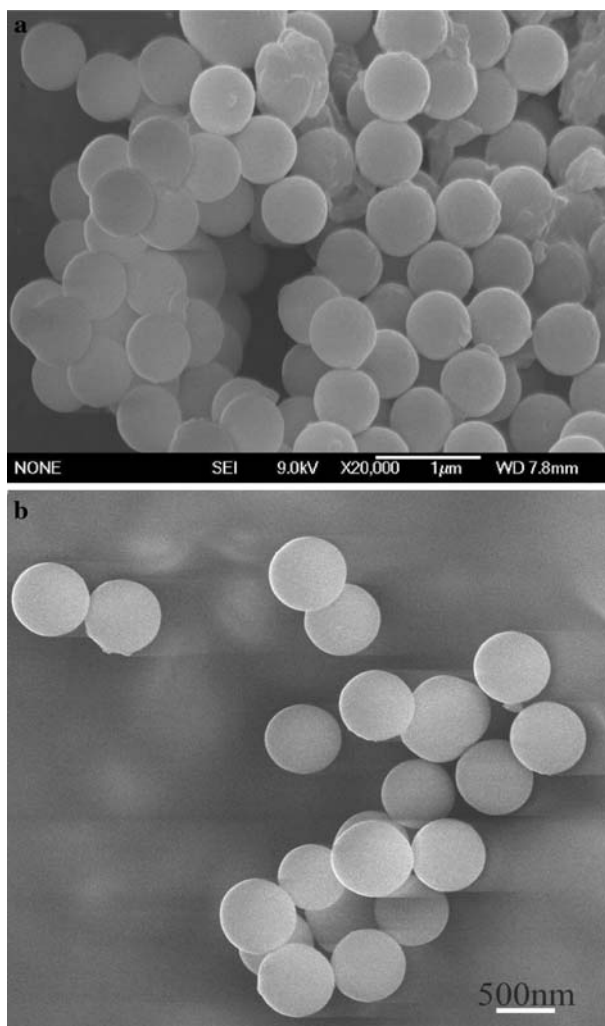


Fig. 1 FE-SEM images of the products. (a) NiS Hollow spheres, (b) PbS hollow spheres.

composed of uniform hexagonal prism structure rods with partly oriented and ordered array in the sections. Further TEM morphology shown in Fig. 3d agrees with the FE-SEM results. Figure 3e shows a representative high-resolution transmission electron micrograph (HRTEM JEOL-2010, all other HRTEM photographs in this article were taken in the same equipment if not especially pointed out) image of a single rod. The clear

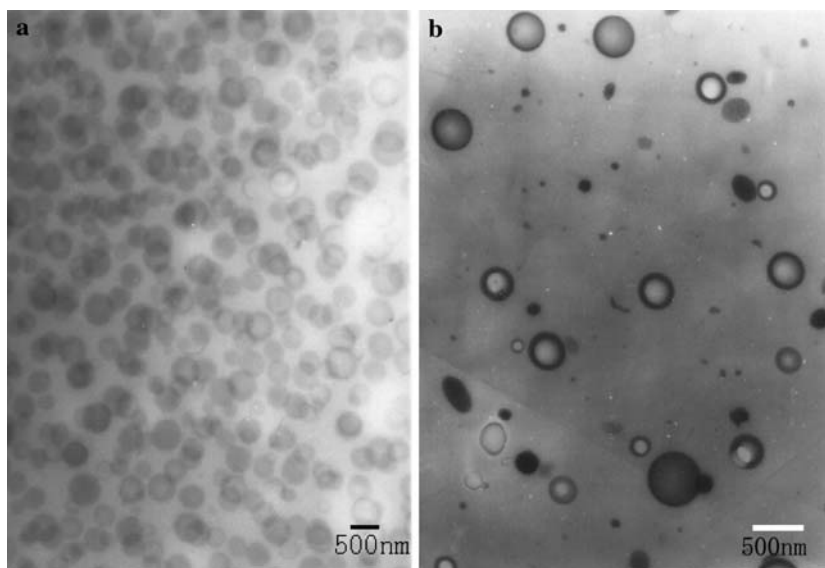
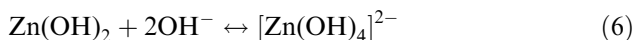
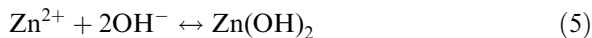


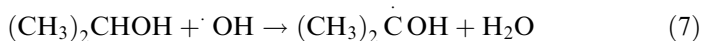
Fig. 2 TEM images of the products. (a) NiS hollow spheres, (b) PbS hollow spheres.

lattice fringes further confirm that the product is a single crystal. The fringe spacing is about 0.52 nm, which is close to the separation between the (0001) lattice planes. This means that the axial direction of the as-prepared sample is perpendicular to the normal direction of the (0001) lattice plane of the hexagonal ZnO. Electron diffraction (ED) pattern (inset in Fig. 3e) also verifies that the as-prepared products are single crystals of hexagonal ZnO.

For the growth process of the as-produced crystals, a possible formation process of ZnO hexagonal prisms was suggested as follows. First, Zn^{2+} salt solution reacts with superfluous OH^- to form transparent solution $\text{Zn}(\text{OH})_4^{2-}$ [44],



Then, the mixed transparent solution with isopropyl alcohol was irradiated by γ -ray. During the radiolysis of aqueous solution, the oxidative species e.g. $\cdot\text{OH}$ was scavenged by isopropyl alcohol (Eq. 7).



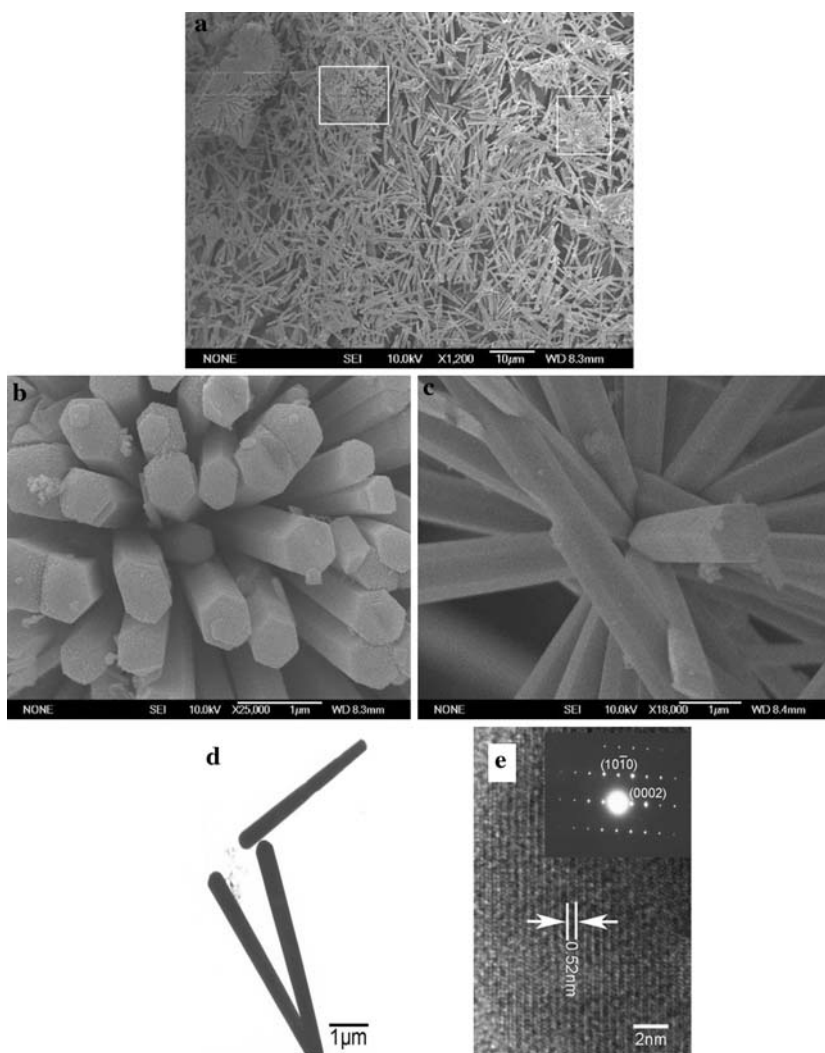
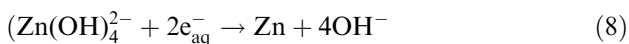


Fig. 3 (a) FESEM image of as-prepared ZnO hexagonal prism. The areas of rectangle are shown enlarged in (b) and (c). (d) TEM image and (e) HRTEM image of ZnO hexagonal prism (inset: ED pattern).

Because pH value of the solution is alkaline, among the remaining reductive species, e_{aq}^- is predominant. e_{aq}^- (its standard redox potential -2.77 V [45]) could easily reduce $Zn(OH)_4^{2-}$ into Zn (its standard redox potential -1.215 V in basic solution) (Eq. 8).



The yielded Zn atoms were very active, while they encountered oxygen (dissolved in the solution and also coming from H_2O_2 dissociation), the oxidative-reductive reaction would take place and produced ZnO (Eq. 9). CTAB is a kind of cationic surfactant, while existing with hydrotropic salt, it can naturally form rod-like micelle (also worm-like shape). During the production of ZnO, the structure-directing agent of CTAB in the solution make the ZnO seed crystal grows along certain orientation to form hexangular prism rods. In the end, the hexangular prism ZnO nanocrystals were obtained.

CdSe HOLLOW STRUCTURES AND HOLLOW NANOSPHERES

Ordered porous materials currently attract considerable interest due to their wide range of applications as catalysts, thermal and acoustic insulators and optical devices [46–48]. Template synthesis is a commonly used tool with technological advantages in the preparation of ordered porous materials [49–51]. Following this, cadmium selenide (CdSe hollow structures and nanospheres were prepared by γ -irradiating soft-template polyvinyl pyrrolidone (PVP) aqueous solution or polyacrylamide (PAM) hydrogel template at room temperature.

All the reagents were of analytical grade and were used without further purification. Sodium selenosulfate (Na_2SeSO_3) could be made by refluxing selenium powders in a sodium sulfite solution [52]. Two kinds of water soluble polymers were used here; they were PVP and PAM hydrogel, respectively.

Solution 1: Solution was prepared by dissolving an appropriate amount of analytically pure $\text{CdCl}_2 \cdot 2\text{H}_2\text{O}$ (1.15 g), PVP (2.5 g), $(\text{CH}_3)_2\text{CHOH}$ (20 mL) and Na_2SeO_3 solution (10 mL) in distilled water.

Solution 2: PAM hydrogel was put into 100 mL aqueous solution containing $\text{CdCl}_2 \cdot 2\text{H}_2\text{O}$ (1.15 g), $(\text{CH}_3)_2\text{CHOH}$ (20 mL) and Na_2SeO_3 solution (0.05 mol dm^{-3} , 10 mL).

All solutions were deaerated by bubbling with pure nitrogen (99.99%) for 20 min. While reaching their swelling equilibrium, solutions were placed in the field of $2.59 \times 10^{15} \text{ Bq } ^{60}\text{Co}$ γ -ray source with a dose of 24.4 KGy. When reactions mostly finished, red and gelatinous products were obtained. The products were dried in vacuum at room temperature, ground to powder, and then washed with distilled water several times till removing all

the by-products. By drying the products in vacuum again at room temperature, we could get the final products CdSe.

The morphology of CdSe hollow structures which are 25~180 nm in pore diameter and 3~7 nm in wall thickness can be clearly shown in the Fig. 4a. From Fig. 4b, we can see that the morphology of hollow nanospheres are 40~50 nm in pore diameter and 3~5 nm in wall thickness.

Possible reasons forming CdSe hollow structures or nanospheres could be explained as follows: First, Se^{2-} can be released homogeneously from SeO_3^{2-} or SeSO_3^{2-} under γ -irradiation. Then, CdSe seed formation occurred by the reaction of Cd^{2+} with freely Se^{2-} :



It should be pointed out that the choice of proper water-soluble polymer as soft template is the key to the successful synthesis of CdSe hollow structures and nanospheres. Organic molecules can alter inorganic microstructures, offering a very powerful tool for the design of novel materials [53]. PVP and PAM around the CdSe nanocrystals prevent the formation of disordered structures, and self-organization of the quantum dots occurring in a controlled fashion as the solubilizing power of the solvent is decreased. Along with the formation of these two- and three-dimensional

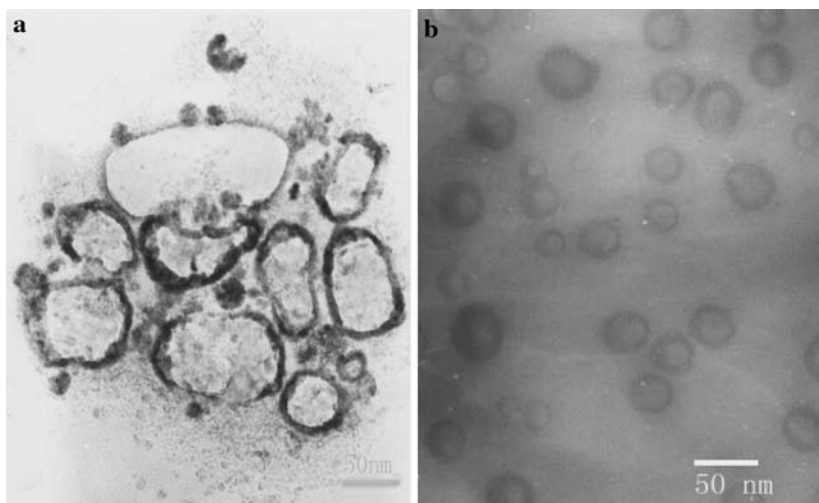


Fig. 4 (a)TEM image of CdSe hollow structures, (b) TEM image of CdSe hollow nanospheres.

networks, CdSe quantum dots can also be joined with specific chemical linkers and formation [54]. However, at the same condition, we could not get CdSe hollow structures and nanospheres in other water-soluble polymer solution.

SINGLE-CRYSTAL COMPASS-SHAPED Mn_3O_4

One of the manganese oxides, Mn_3O_4 , has been widely used as the main source of ferrite materials, which have extensive applications in electronic and information technologies. This material has also attracted interest as an active catalyst for the reduction of nitrobenzene or oxidation of methane [55–57]. Herein, we provide a novel approach to prepare monodisperse and uniform single-crystal compass-shaped Mn_3O_4 nanocrystals in a surfactant-assisted solution by γ -ray.

In a typical experiment, analytically pure $\text{MnSO}_4 \cdot \text{H}_2\text{O}$ (0.846 g), CTAB 2.0 g and isopropyl alcohol (15 mL) were dissolved into 50 mL distilled water under intensively stirring for 0.5 h at room temperature. The mixed solution was irradiated in the field of a 2.22×10^{15} Bq ^{60}Co γ -ray source with the absorption dose of 80 kGy at the dose rate of 50 Gy/min. After irradiation, the black precipitates were collected through centrifugation, placed in air for 24 h, washed with distilled water and ethanol several times, and dried in air at room temperature. The conversion ratio of the reaction was about 20%.

TEM and HRTEM images of the sample are shown in Fig. 5. TEM images (at low magnification Fig. 5a and at high magnification Fig. 5b) reveal that the sample consists entirely of monodisperse and uniform compass-shape with 80 nm in middle width and 200 nm in length. Figure 5c shows a representative HRTEM image of a single nanocompass. The clear lattice fringes further confirm that the nanocompass is a single crystal. The fringe spacing is about 0.49 nm, which is close to the separation between the (101) lattice planes. This indicates that the axial direction of the as-prepared nanocompass is perpendicular to the normal direction of the (101) lattice plane of the tetragonal hausmannite Mn_3O_4 . Electron diffraction (ED) pattern (inset in Fig. 5c) obtained from a single nanocompass also confirms that the as-prepared products are single crystals of tetragonal hausmannite Mn_3O_4 , which is in agreement with XRD pattern result.

A possible formation process of the compass-shaped Mn_3O_4 nanocrystals was suggested according to the designed route. The hydrated electron and the hydrogen atom, which created during the radiolysis of aqueous solution, were strong reductive particles. They could reduce Mn^{2+} into Mn atoms. Meanwhile, some oxidative particles such as $\cdot\text{OH}$ were scavenged by isopropanol. So, Mn^{2+} was mainly reduced by the hydrated electron (Eq. 12):

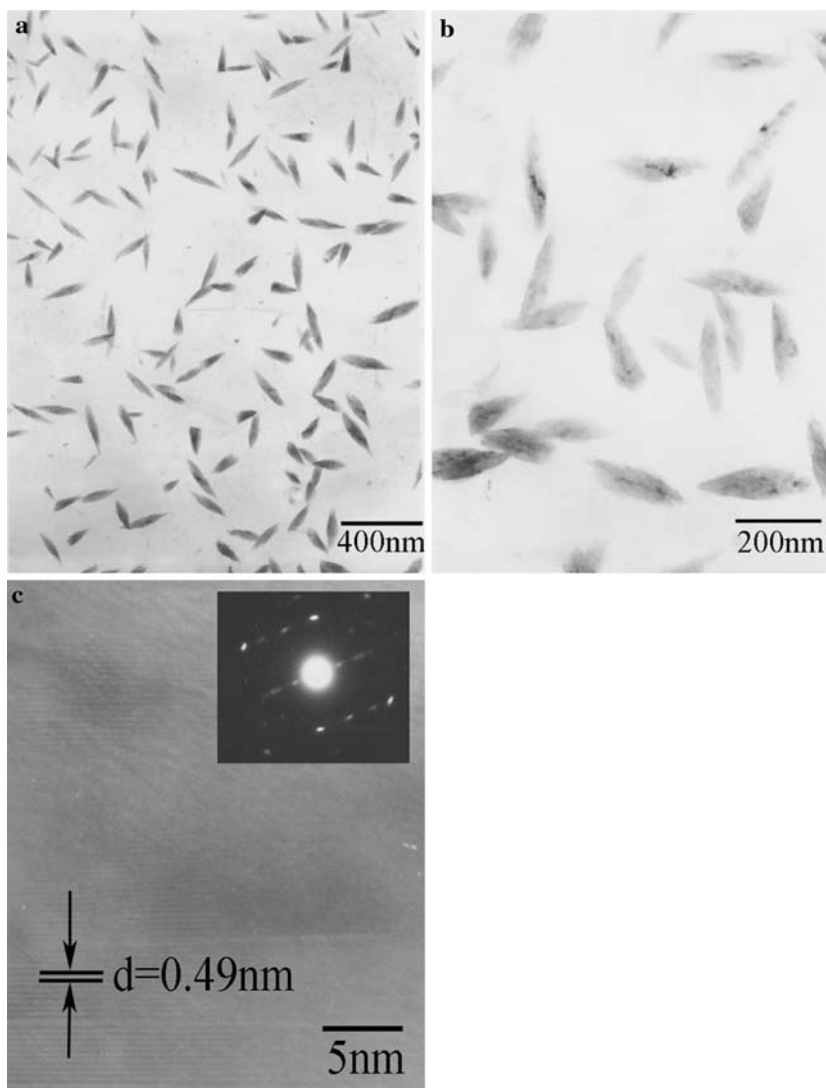


Fig. 5 TEM images of the as-prepared compass-shaped Mn_3O_4 (a) at low magnification; (b) at high magnification. (c) HRTEM image of a single as-prepared Mn_3O_4 nanocompass.



The newly-yielded Mn atoms were very active, so they only could exist in the reducing conditions. During the reduction of Mn, a layer-shaped

structure existed in the CTAB solution could be attached only along certain direction by the hydrated electrons. Thus, it was possible that the Mn particles grew in a certain shape. When these Mn particles with shaped were treated in air, they were quickly oxidized by oxygen in the air. So, the compass-shaped Mn_3O_4 nanocrystals could be obtained.



The whole reactions could be regarded as chain reactions. While the little yield of Mn gained, Mn was oxidized into Mn_3O_4 at once, equation 2 might go persistently. So, the yield of the reaction was higher than estimated.

MONODISPERSE ZnS NANOSPHERES

There is considerable interest on the fabrication of uniform-sized nanoballs. As one of promising materials, Zinc sulfide (ZnS), a direct wide band gap transparent semiconductor, is used in photonics research [58–60], and also has a variety of applications such as electroluminescent devices, solar cells, and other optoelectronic devices [61–63]. Following the paragraph, monodisperse ZnS nanoballs were synthesized through γ -irradiating PVP-assisted aqueous solution.

Irradiating solutions were prepared by dissolving an appropriate amount of analytically pure 1.36 g of ZnCl_2 , 2.48 g of $\text{Na}_2\text{S}_2\text{O}_3 \cdot 5\text{H}_2\text{O}$, 0.75 g of PVP and 50 mL of distilled water. After vigorously stirred about 1h at room temperature, solutions were then irradiated in the field of $2.59 \times 10^{15} \text{Bq } ^{60}\text{Co}$ γ -ray source with a dose of 133.06 KGy. The white powders obtained were collected by centrifugation, washed with distilled water and ethanol several times till the final products had high purity.

FESEM of the products, which obtained for 24 h irradiating time under ambient pressure and at room temperature, was shown in Fig. 6. From this, we could find that the products were composed of the multi-layers monodisperse nanoballs with average diameter about 120 nm. The ZnS nanoballs are randomly and homogeneously distributed in all areas. The size and morphology of the nanoballs were further examined by TEM. By changing irradiation time, we investigate the size-control of these ZnS nanoballs. The irradiation time was controlled for 6, 18, 24 and 30 h, and corresponding to the radiation doses 66.53 KGy, 99.79 KGy, 133.06 KGy and 166.33 KGy, respectively. The experimental results were shown in Fig. 7. The longer the irradiation time was, the larger the size of ZnS nanoballs formed was. The uniformity of nanoballs changed with the radiation time while keeping other conditions the same. In this case, it's

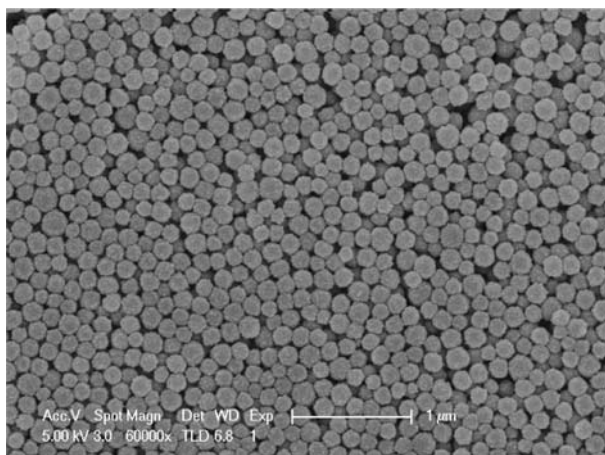
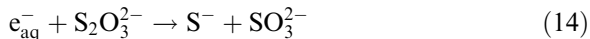


Fig. 6 FESEM image of as-grown ZnS nanoballs.

found that the uniformity of the nanoballs was better when the radiation time was 24 h.

The possible reaction processes for the formation of ZnS nanoballs could be described as follows:



And then, the growth of the seeds continues whether the ZnS grows on the seeds (growth in a supersaturated solution), or by the process of Ostwald ripening whereby larger seeds grow at expense of the smaller ones [64, 65]. Generally speaking, if the main process of the nanoparticle growth is Ostwald ripening, there is change in the nanoparticle size distribution with reaction time. For the ZnS growth in this case, it's believed that the process of Ostwald ripening is dominant. Because when the irradiation time was altered, the size of ZnS nanoballs was changed.

CONCLUSION

In summary, sulfide and oxide semiconductor nano- and micro-structures were successfully synthesized by controlled growth via gamma-irradiation route. This radiation synthetic pathway provides an important

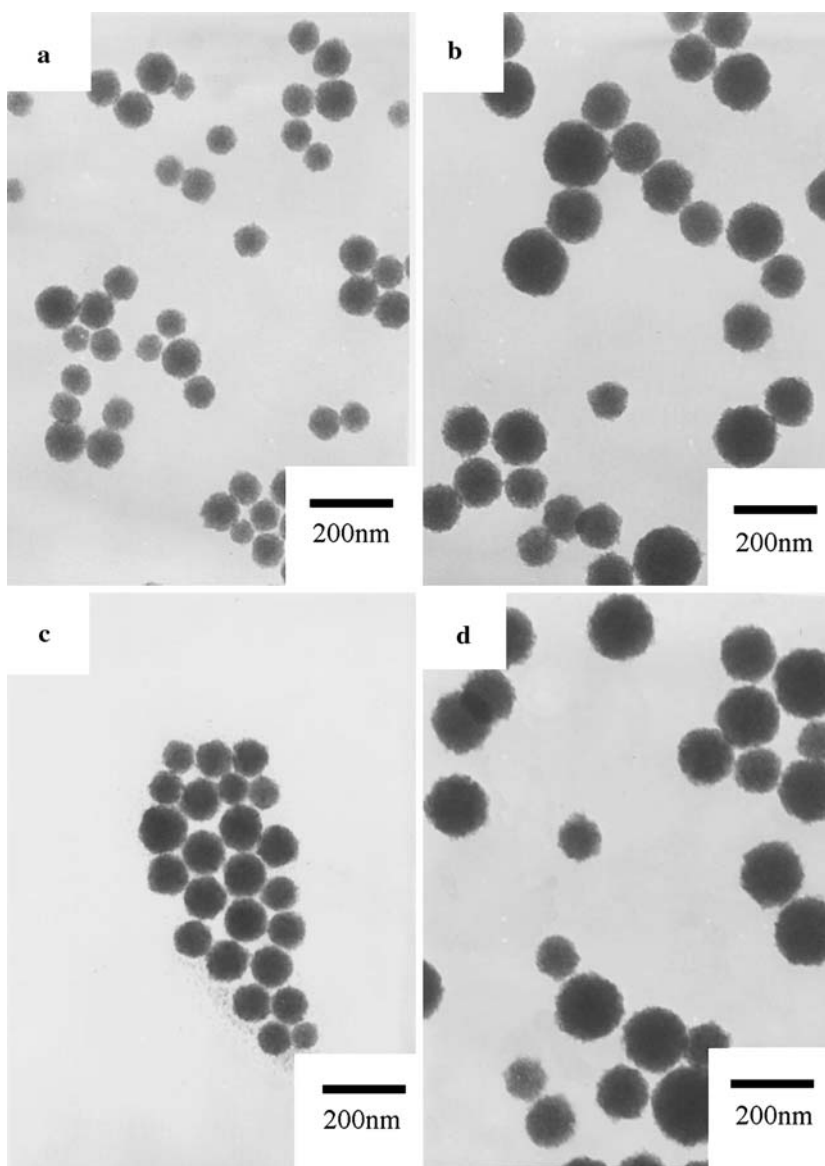


Fig. 7 TEM images of ZnS nanoballs. The irradiation time is 6h (a), 12h (b), 24h (c), and 48h (d), respectively.

example of semiconductor materials with designed morphology. Compared with other synthesis approaches, the synthetic method presented here is simpler and more effective. The present results demonstrate the potential feasibility to synthesize substantive inorganic semiconductor compounds under mild conditions, showing that gamma-irradiation route is a promising route for rationally and structurally designing nanomaterials. It also may stimulate technological interest and prospect many applications in material fields.

ACKNOWLEDGMENTS

This work was financially supported by the grants of National Science Foundation of China (No.20621061, 20473082), and the Anhui Provincial Natural Science Foundation (070414195).

REFERENCES

1. E. Menard, K. J. Lee, D. Y. Khang, R. G. Nuzzo, and J. S. Rogers (2004). *Appl. Phys. Lett.* **84**, 5398.
2. B. A. Ridley, B. Nivi, and J. M. Jacobson (1999). *Science* **286**, 746.
3. X. Duan, C. Niu, V. Sahl, J. Chen, J. W. Parce, S. Empedocles, and J. L. Goldman (2003). *Nature* **425**, 274.
4. A. P. Alivisatos (1996). *Science* **271**, 933.
5. A. P. Alivisatos, P. F. Barbara, A. W. Castleman, J. Chang, D. A. Dixon, M. L. Kline, G. L. Melendon, J. S. Miller, M. A. Ratner, P. I. Rosicky, S. I. Stupp, and M. I. Thompson (1998). *Adv. Mater.* **10**, 1297.
6. Y. Xia, P. Yang, Y. Sun, Y. Wu, B. Mayers, B. Gates, Y. Yin, F. Kim, and H. Yan (2003). *Adv. Mater.* **15**, 353.
7. M. Nirmal and L. Brus (1999). *Acc. Chem. Res.* **32**, 407.
8. G. Markovich, C. P. Collier, S. E. Henrichs, F. Remacle, R. D. Levine, and J. R. Heath (1999). *Acc. Chem. Res.* **32**, 415.
9. J. Hu, T. W. Odom, and C. M. Lieber (1999). *Acc. Chem. Res.* **32**, 435.
10. M. H. Huang, S. Mao, H. Feick, H. Yan, Y. Wu, H. Kind, E. Weber, R. Russo, and P. Yang (2001). *Science* **292**, 1897.
11. Z. W. Pan, Z. R. Dai, and Z. L. Wang (2001). *Science* **291**, 1947.
12. X. Y. Kong, Y. Ding, R. Yang, and Z. L. Wang (2004). *Science* **303**, 1348.
13. Y. Wang, X. Jiang, and Y. Xia (2003). *J. Am. Chem. Soc.* **125**, 16176.
14. D. Battaglia, J. J. Li, Y. Wang, and X. Peng (2003). *Angew. Chem. Int. Ed.* **42**, 5035.
15. D. J. Milliron, S. M. Hughes, Y. Cui, L. Manna, J. Li, L. W. Wang, and A. P. Alivisatos (2004). *Nature* **430**, 190.
16. N. A. Melosh, A. Boukai, F. Diana, B. Gerardot, A. Badolato, P. M. Petroff, and J. R. Heath (2003). *Science* **300**, 112.
17. Z. W. Pan, Z. R. Dai, and Z. L. Wang (2002). *Appl. Phys. Lett.* **80**, 309.
18. F. Gao, Q. Lu, X. Liu, Y. Yan, and D. Zhao (2001). *Nano. Lett.* **1**, 743.
19. W. Xun, X. M. Sun, D. P. Yu, B. S. Zou, and Y. D. Li (2003). *Adv. Mater.* **15**, 1442.
20. A. M. Morales and C. M. Lieber (1998). *Science* **279**, 208.

21. K. K. Caswell, J. N. Wilson, U. H. F. Bunz, and C. J. Murphy (2003). *J. Am. Chem. Soc.* **125**, 13914.
22. Z. P. Qiao, Y. Xie, J. G. Xu, and Y. T. Qian (1999). *J. Colloid. Interface Sci.* **214**, 459.
23. Y. Yin, X. Xu, X. Xia, X. Ge, and Z. Zhang (1998). *Chem. Commun.* **8**, 941.
24. Y. Yin, X. Xu, X. Ge, X. Xia, and Z. Zhang (1998). *Chem. Commun.* **16**, 1641.
25. S. H. Yu, Y. S. Wu, and J. Yang (1998). *Chem. Mater.* **9**, 2312.
26. Y. Hu, W. M. Chen, and J. F. Chen (2003). *Mater. Lett.* **57**, 1312.
27. Y. Hu, J. F. Chen, and W. M. Chen (2003). *Adv. Mater.* **15**, 726.
28. Y. Hu, J. F. Chen, X. Xue, T. W. Li, and Y. Xie (2005). *Inorg. Chem.* **44**, 7280.
29. Y. Hu, J. F. Chen, and W. M. Chen (2005). *Mater. Lett.* **59**, 234.
30. Y. Hu, J. F. Chen, and W. M. Chen (2004). *Mater. Lett.* **58**, 2911.
31. Y. Hu, J. F. Chen, and W. M. Chen (2003). *Mater. Lett.* **57**, 3137.
32. (a) Y. Hu, J. F. Chen, X. Xue and T. W. Li (2006). *Mater. Lett.* **60**, 383. (b) X. Xue, J. F. Chen and Y. Hu (2007). *Mater. Lett.* **61**, 115.
33. D. L. Wilcox, M. Berg, T. Bernat, D. Kellerman, J. K. Cochran (eds.), *Materials Research Society proc.* (Materials Research Society, Pittsburgh, PA. 1995), Vol. 372.
34. Z. Zhong, Y. D. Yin, B. Gate, and Y. N. Xia (2000). *Adv. Mater.* **12**, 206.
35. X. D. Wang, W. L. Yang, Y. Tang, Y. J. Wang, Gao Z. (2002) *Chem. Commun.* 2161.
36. N. Kawahashi and H. Shiho (2000). *J. Mater. Chem.* **10**, 2294.
37. R. Janes, A. D. Stevens, and M. C. R. Symons (1989). *J. Chem. Soc. Araday Trans.1* **85**, 3973.
38. A. Charlesby and M. Ross (1953). *Nature* **171**, 1153.
39. L. A. Wall and D. W. Brown (1956). *J. Res. Nat. Bur. Stand* **57**, 131.
40. P. V. Braun and S. I. Stupp (1999). *Mater. Res. Bull.* **34**, 463.
41. Y. Cui and C. M. Lieber (2001). *science* **291**, 851.
42. W. I. Park, G. C. Yi, M. Kim, and S. J. Pennycook (2003). *Adv. Mat.* **15**, 526.
43. X. Duan, Y. Huang, Y. Cui, J. Wang, and C. M. Liber (2001). *Nature* **409**, 66.
44. H. Zhang, D. R. Yang, Y. J. Ji, X. Y. Ma, and D. L. Que (2004). *J. Phys. Chem. B* **108**, 3957.
45. J. W. T. Spinks, R. J. Wood *An Introduction to Radiation Chemistry.* (John Wiley & Sons Inc, 1976).
46. M. P. Harold, C. Lee, A. J. Burggraaf, K. Kaizer, and V. T. Zaspalis (1994). *MRS Bull* **19**, 34.
47. E. Litovsky, M. Shapiro, and A. Shavit (1996). *J. Am. Ceram. Soc.* **79**, 1366.
48. Y. Xia, B. Gate, Y. Yin, and Y. Lu (2000). *Adv. Mater.* **12**, 693.
49. C. T. Kresge, M. E. Leonowicz, W. J. Roth, J. C. Vartuli, and J. S. Beck (1992). *Nature* **359**, 710.
50. S. A. Bagshaw, E. Prouzet, and T. J. Pinnavaia (1995). *Science* **269**, 1242.
51. D. Zhao, G. Huo, J. Feng, B. F. Chmelka, and G. D. Stucky (1998). *J. Am. Ceram. Soc.* **120**, 6042.
52. P. Pramanick and R. N. Bhattacharye (1982). *J. Solid State Chem.* **44**, 425.
53. S. I. Stupp and P. V. Braun (1997). *Science* **277**:1242.
54. X. Peng, T. E. Wilson, A. P. Alivisatos, and P. G. Schultz (1997). *Angew. Chem. Int. Ed.* **36**, 145.
55. E. Grootendorst, Y. Verbeek, and V. Ponce (1995). *J. Catal.* **157**, 706.
56. L. Chen, T. Horiuchi, and T. Mori (2001). *Appl. Catal. A: Gen* **209**, 97.
57. E. R. Stobbe, B. A. D. Boer, and J. W. Geus (1999). *Catal. Today* **47**, 161.
58. S. Kishimoto, A. Kato, A. Naito, Y. Sakamoto, and S. Iida (2002). *Phys. Stat. Sol.* **1**, 391.
59. L. Sun, C. Liu, C. Liao, and C. Yan (1999). *J. Mater. Chem.* **9**, 1655.
60. X. Jiang, Y. Xie, J. Lu, L. Zhu, W. He, and Y. Qian (2001). *Chem. Mater.* **13**, 1213.

61. M. Bredol and J. Merichi (1998). *J. Mater. Sci.* **33**, 471.
62. P. Calandra, M. Gofferdi, and V. T. Liveri (1999). *Colloids Surf. A* **9**, 160.
63. T. V. Prevenslik (2000). *J. Lumin.* **87**, 1210.
64. A. S. Kabalnov and E. D. Shchukin (1992). *Adv. Colloid Interface Sci.* **38**, 69.
65. P. Taylor (1995). *Colloids Surf. A* **99**, 175.